

***Ab initio* calculation of binding and diffusion of a Ga adatom on the GaAs (001)-*c*(4×4) surface**

J. G. LePage

*Air Force Research Laboratory, Wright Patterson Air Force Base, Ohio 45433-7707
and Department of Physics, The Ohio State University, Columbus, Ohio 43210*

M. Alouani

*IPCMS, Université Louis Pasteur, 13, rue du Loess, Strasbourg, France
and Department of Physics, The Ohio State University, Columbus, Ohio 43210*

Donald L. Dorsey

Air Force Research Laboratory, Wright Patterson Air Force Base, Ohio 45433-7707

J. W. Wilkins

Department of Physics, The Ohio State University, Columbus, Ohio 43210

P. E. Blöchl

IBM Research Division, Zürich, Switzerland

(Received 29 August 1997; revised manuscript received 6 April 1998)

We have investigated the diffusive behavior of a single Ga adatom on the GaAs(100)-*c*(4×4) surface by means of the local-density approximation and the all-electron projector augmented wave (PAW) method. The ground-state geometry of the GaAs(100)-*c*(4×4) surface is determined using PAW and is found to agree with experiment and previous calculations. The binding energy for a lone Ga adatom on this reconstruction is calculated as a function of surface position. Based on these data we have identified three relatively stable adsorption sites. In order of increasing energy these sites are site 1 at the center of the missing dimer position; site 2 between the dimer rows and adjacent to a center dimer; and site 3 between the dimer rows, adjacent to an edge dimer. The surface diffusion activation energies have also been identified; the smallest is 0.14 eV for the 3→2 transition, and the largest is 0.45 eV for 2→3. Kinetic Monte Carlo simulations incorporating these data indicate that diffusion on this surface takes place primarily through diffusion pathways that pass through the strongest binding site (site 1). This site effectively controls diffusion in directions both parallel and perpendicular to the dimer rows. [S0163-1829(98)07627-9]

I. INTRODUCTION

We present the results of an *ab initio* investigation of the behavior of an adatom on a semiconductor surface. More specifically, we compute the energetics of the diffusion of a lone Ga adatom on the GaAs(100)-*c*(4×4) reconstructed surface. From a practical perspective, as the dimensions of semiconductor devices continually decrease, the need for a better understanding of the processes that occur on surfaces during device growth becomes increasingly acute. In particular, detailed knowledge of surface diffusion processes on the *c*(4×4) surface reconstruction relates directly to the manufacture of nonstoichiometric GaAs films.

In recent years, in an effort to guide the development of thin-film growth technology, a number of groups have made theoretical studies of vapor phase epitaxy.¹ Unfortunately, most current models require the knowledge of a large number of input parameters whose precise values are difficult to determine via experiment. For example, lattice Monte Carlo² simulations require that the desorption, adsorption, and surface diffusion energetics be understood at the atomic level.³ However, the values of the relevant activation energies are generally not known accurately. In the absence of good experimental data, Monte Carlo theorists often resort to rough

approximations designed to produce a final simulation that is in reasonable agreement with the known growth morphology. As a result, current lattice Monte Carlo simulation programs are more useful as qualitative guides than as quantitative predictors.^{2,4} On the other hand, Monte Carlo techniques are capable of modeling, however imprecisely, the molecular-beam epitaxy (MBE) deposition of several complete monolayers. If the relevant kinetic Monte Carlo parameters could be determined, then a well-constructed kinetic Monte Carlo algorithm would yield quantitative accuracy.

One of the purposes of this study is to expand the predictive capabilities of kinetic Monte Carlo simulations by using *ab initio* techniques to generate diffusion parameters. Several groups have conducted similar calculations for the Si(001)-(2×1) and the GaAs(001)-(2×4) reconstructed surface.⁵ Unfortunately, *ab initio* simulations, while capable of high accuracy, are so computationally demanding that only simulations involving rather small systems (on the order of 100 atoms) over very small times (a few picoseconds) are currently feasible. Here we do not attempt an actual simulation of growth but instead calculate the self-consistent potential energy surface for a single isolated adatom. An analysis of this data will yield the diffusion activation barriers for the dilute (low adatom concentration) case.

II. DETAILS OF THE CALCULATIONS

All *ab initio* calculations in this study were done using the projector augmented wave (PAW) method.⁶ The PAW method is a new formalism that combines features of both the augmentation methods [e.g., linear augmented plane wave (LAPW) (Refs. 7 and 8)] and the pseudopotential method.⁹ Like the LAPW method, the PAW method uses a mixed basis set incorporating both plane waves and atomic wave functions. However, unlike the LAPW method, the PAW basis set includes an additional set of *pseudoatomic* wave functions, which are the solutions of Schrödinger's equation for a *pseudized* atomic potential. The use of atomic wave functions in the basis set allows us to deal naturally with *d* and *f* orbitals, while the pseudo-atomic wave functions provide a convenient mathematical bridge between the plane waves and the atomic wave functions. PAW is implemented in the context of standard density-functional theory and uses the local-density approximation. The exchange-correlation potential is approximated by the Perdew-Zunger parameterization of Ceperly and Adler's data.¹⁰ The Car-Parrinello¹¹⁻¹⁴ molecular dynamics algorithm is used to determine the electronic structure and ionic geometry. Further details of the PAW method can be found in Ref. 6.

Although the PAW method is a fairly recent innovation, the method has been used successfully in a number of studies.¹⁵⁻¹⁸ Additionally, a recent comparison study concluded that the structural properties of several representative covalent, ionic, and metallic materials were calculated equally well by the PAW, LAPW, and pseudopotential methods.¹⁹ In order to test the reliability of the particular gallium and arsenic basis set parameters used in our study, we calculated both the equilibrium lattice constant for bulk GaAs and the ground-state geometry of the GaAs (001)-*c*(2×2) reconstructions. In both cases, the agreement with the available experimental and theoretical data is good.²⁰⁻²²

The first step in the surface calculations is the determination of the electronic structure of the initial geometry. Once this has been done, the atoms are released from their fixed positions and allowed to move under the influence of the *ab initio* calculated forces. In all cases, the iteration time step was 10 atomic units (0.24 fs). Initially, an automatic annealing routine is used to optimize the geometry. If the total energy of the system increases during the simulation then this annealing routine turns on a large effective friction. When the total energy starts to decrease, a small amount of friction is applied and this amount is reduced after each successive iteration during which the total energy decreases. This run ends automatically when the total energy changes by no more than 10^{-5} hartree over 10 iterations. After the automatic annealing procedure has finished, a zero-friction run is conducted for a total of 1000 atomic time units (24 fs or 100 iterations). The purpose of this zero-friction run is to verify that the automatic annealing procedure has not stopped the simulation prematurely. In general, if the total energy shows a variation of less than an energy convergence criterion δE during a zero-friction run, then the total energy is considered to be converged. In most cases, δE is set to 1 mH. However, during particularly critical calculations (such as the determination of the total energy when a Ga adatom is

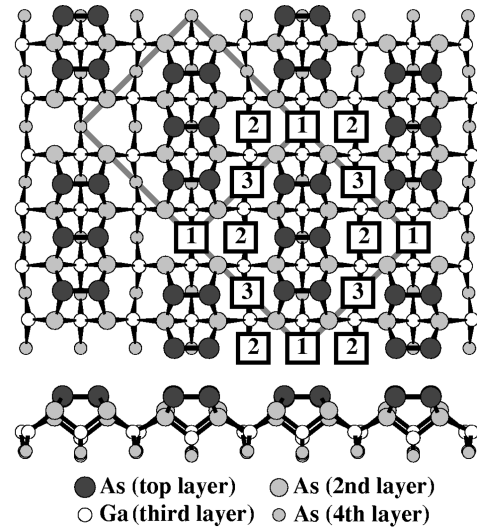


FIG. 1. Top (above) and side view (below) of the calculated geometry of the GaAs(001)-*c*(4×4) surface. Two unit cells (each bounded by a wide gray line) are shown for reference. The positions of the three calculated Ga bonding sites are indicated by the numbered squares.

at a binding site or at a saddle point between binding sites), δE is set to 0.01 mH.²³ If the energy fluctuations during a zero-friction run are greater than δE , then the simulation is started up again, this time with a small constant friction. This low-friction simulation is allowed to continue until the fluctuations in the total energy settle down to less than δE . A further zero-friction run follows, and this low-friction/zero-friction procedure repeats until convergence is confirmed. In some especially difficult cases, the total simulation time has exceeded 1000 iterations. As a final check on convergence, the forces at the end of the simulations were examined.²⁴ Ground-state geometries for the surface-adatom system when the Ga adatom was at a binding site or at a saddle point exhibited residual forces of less than 0.02 eV/Å.

The geometry of GaAs(001)-*c*(4×4) structure is shown in Fig. 1. The plane-wave cutoff for the wave functions is 10 Ry. The *k*-point integration is performed using 4 *k*-points in the plane of the surface. Written in terms of the two-dimensional (2D) reciprocal lattice vectors of the *c*(4×4) surface unit cell, these points are (0,0), (1/2,1/2), (1/2,0), and (0,1/2). Table I gives convergence data with respect to vacuum spacing, slab thickness, plane-wave cutoff, and number of *k* points for the GaAs(001)-*c*(4×4) structure. Based on these data we estimated the error in the difference between total energies of different structures to be on the order of 25 meV.

III. GaAs(100)-*c*(4×4) RECONSTRUCTED SURFACE

The GaAs(100)-*c*(4×4) surface was chosen for this study for three reasons. First, surfaces growing in the *c*(4×4) regime typically exhibit rough morphologies and do not produce the reflection high-energy diffraction oscillations seen during the growth of smooth epitaxial layers. This makes the *c*(4×4) surface a model candidate for the calculation of improved MBE simulation parameters.

Second, this reconstruction has an extremely high As con-

TABLE I. Convergence tests for the calculation of the relative binding energies of a Ga adatom on the GaAs(100)- $c(4 \times 4)$ with respect to the system size parameters: slab thickness, number of k points, plane-wave cutoff, and vacuum spacing between the superlattices. In the main calculation the parameters used were: (1) 10 Ry plane-wave cutoff, (2) four k points, (3) vacuum spacing of 9.5 Å, and (4) four-layer-thick slab. In terms of the 2D reciprocal lattice vectors of the $c(4 \times 4)$ cell, the four- k -point set is (0,0), (1/2,1/2), (1/2,0), and (0,1/2). The larger 16 k -point set was obtained by quadrupling the area of the original unit cell. Time-reversal symmetry reduces the original set of 16 to 10: (0,0), (0,1/4), (0,1/2), (1/4,0), (1/4,1/4), (1/4,1/2), (1/2,0), (1/2,1/4), (1/2,1/2), and (1/4,-1/4). ΔE_b is the difference between the adatom binding energy at two different sites on the surface. $\delta(\Delta E_b)$ is the change in the calculated ΔE_b that results from an increase in a given system size parameter.

| | k points 4 per BZ \rightarrow 16 per BZ | Vacuum spacing 6.9 Å \rightarrow 9.5 Å | Slab thickness 4 layers \rightarrow 8 layers | Plane-wave cutoff 10 Ry \rightarrow 20 Ry |
|----------------------|------------------------------------------------|---------------------------------------------|---------------------------------------------------|------------------------------------------------|
| $\delta(\Delta E_b)$ | 4 meV | 4 meV | 11 meV | 21 meV |

tent. In fact, this reconstruction is known experimentally to occur only under conditions of high As overpressure.^{25,26} Films grown in this regime have an excess of 1–2 % As.²⁵ Such films have a couple of interesting properties.^{27,28} They have very high resistivity, making them ideally suited as a substrate since this high resistance nearly eliminates interaction between neighboring devices. This allows for much increased device density. Also, As-rich GaAs films have excellent crystallinity and good surface morphology so subsequent GaAs layers of high quality can be grown on top of these films. The $c(4 \times 4)$ reconstruction is quite large. As a result, the calculations provide a large-scale test of both the theoretical method (PAW) and of the robustness of its computer implementation.

Our strategy for determining the diffusion characteristics of a Ga adatom on the $c(4 \times 4)$ surface is straightforward. We begin with a simple repeated slab (superslab) model composed of a vacuum region and a few atomic layers of GaAs. Our particular unit cell is composed of five atomic layers of GaAs (eight atoms in each layer) capped on the top by six As atoms and on the bottom by four Ga atoms. The vacuum region is about 6 ML thick. The six As atoms on the top of the slab form the three surface dimers seen in the $c(4 \times 4)$ reconstruction while the four Ga atoms on the bottom side of the slab form the outermost layer of a $c(2 \times 2)$ reconstructed surface. The non-polar and semiconducting $c(2 \times 2)$ reconstruction is used to passivate the bottom side of the slab. The total height of the unit cell (crystal slab and vacuum layer) is 16.95 Å. The transverse lattice constants are taken to be equal to the experimental bulk lattice constant.²¹

Such a unit-cell geometry will model the real surface accurately only if the bottom and top surfaces do not interact strongly with each other. This condition can usually be met if the bottom surface has the following characteristics. First, the surface should contain no partially filled bonding orbitals, which might result in hard-to-predict effects on the electronic structure of the complete structure. Second, the surface must be nonpolar in order to lessen electrostatic interactions between surfaces. The $c(2 \times 2)$ reconstruction satisfies both these conditions. In addition, it has the added feature that it is a very shallow reconstruction; the atoms immediately below this reconstructed surface are very close to their bulk equilibrium positions.

The initial geometries for both the $c(2 \times 2)$ and $c(4 \times 4)$

reconstructions were taken from the available experimental and theoretical data. In the case of the GaAs(001)- $c(2 \times 2)$ reconstruction, initial coordinates were supplied by Froyen.²² For the GaAs(001)- $c(4 \times 4)$ reconstruction, the STM data of Biegelsen *et al.*²⁵ was used as a rough guide for the initial geometry.

Prior to the main series of simulations, we first optimize the geometry of the terminating GaAs(001)- $c(2 \times 2)$ surface, in a separate series of calculations. The initial geometry for these simulations is a seven layer slab capped on both sides by an initial guess for the geometry of the $c(2 \times 2)$ reconstruction. The total height of the (slab)+(vacuum layer) is 14.125 Å. The transverse lattice constants are taken to be the bulk lattice constant. Once the electronic ground state had been calculated for the initial geometry, all atoms in this system are allowed to relax to their ground state positions. Once determined, this optimized $c(2 \times 2)$ geometry is grafted onto the bottom surface of the unit cell used in the main series of calculations. In the main series of simulations, the 12 atoms (1 ML of As and $\frac{1}{2}$ ML of Ga) in the $c(2 \times 2)$ terminating surface are held fixed in their equilibrium positions. The geometry of the GaAs(001)- $c(4 \times 4)$ reconstruction is calculated using the same techniques as those for the terminating GaAs(001)- $c(2 \times 2)$ reconstruction.

Next, an adatom is introduced at a position (x,y) above the surface. Within the constraint that the (x,y) coordinates of the adatom be held fixed, all atoms except those in the terminating $c(2 \times 2)$ layer are allowed to settle into their equilibrium positions. By repeating this procedure for 41 points within the real-space irreducible zone of the surface, we map out the total energy of the structure as a function of adatom position: $E_{\text{adatom}}(x,y)$. The 41 points in the sampling grid form a rectangular grid with a spacing of slightly less than 1 Å. The principal results of our *ab initio* calculations are shown in Fig. 2. The energy surface shown is a cubic spline fit to the original data. The density of points on the interpolated map is nine times the density of the original map. The interpolation is constrained so that coincident (x,y) points on the original and interpolated maps have the same energy value.

Of course, the true minima of the potential energy surface do not in general fall on the original grid points. To produce the correct binding energies and sites, we placed the adatom near the suspected binding sites and let it relax uncon-

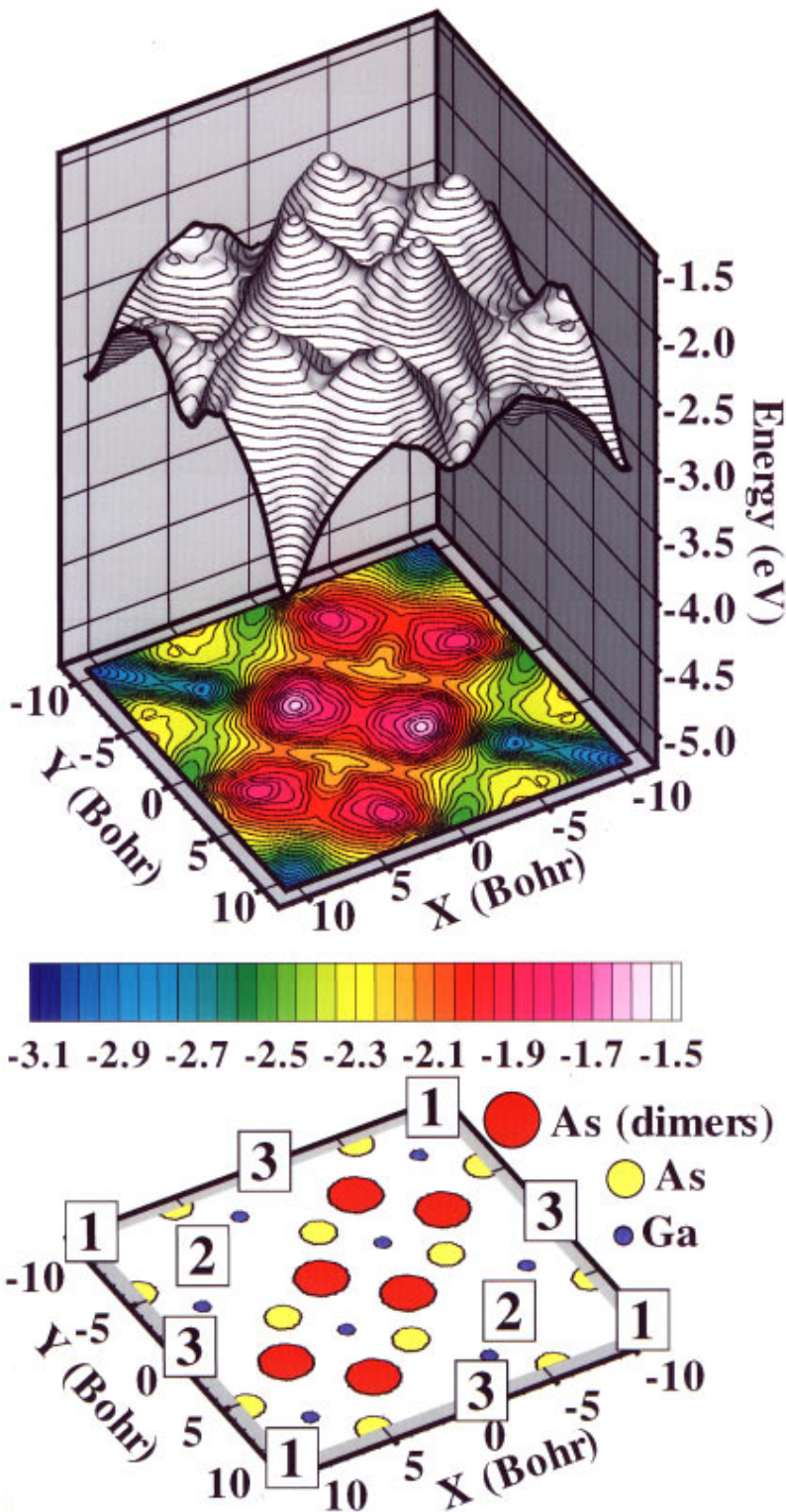


FIG. 2. (Color) The energy of a Ga adatom on the GaAs(001)- $c(4\times 4)$ reconstructed surface as a function of position. We investigated the behavior of an isolated Ga adatom on the GaAs(001)- $c(4\times 4)$ surface. Shown below is a schematic diagram of a GaAs(001)- $c(4\times 4)$ unit cell. In this diagram the larger atoms are closer to the surface. The diagram above shows the potential energy of a Ga adatom as a function of position on the surface. The contour lines on the three-dimensional rendering correspond to those on the two-dimensional (color-coded) contour graph below. The interval between contour lines is 50 meV. The location of the bonding sites can be deduced directly from this diagram. The bonding sites are labeled in order of decreasing bond strength. The most favorable bonding site (site 1) is located at the corners of the unit cell. Activation barriers to diffusion can be determined from this graph.

strained. The resultant sites are indicated in Fig. 1. With respect to the energy of a system composed of the surface plus an *isolated* Ga atom, the energy of the surface-adatom system when the adatom is bound at site 1 is ($E_{\text{adatom}} = -3.04$ eV). Site 1 is at the center of the missing dimer position. The energy at site 2 (between the dimer rows and adjacent to a center dimer) is $E_{\text{adatom}} = -2.85$ eV. The energy at site 3 (between the dimer rows and adjacent to an edge dimer) is $E_{\text{adatom}} = -2.54$ eV. the energies of the saddle

points between the binding sites. The saddle point *a*, between sites 1 and 2, has an energy of $E_{\text{adatom}} = -2.70$ eV. The saddle point *b*, between sites 2 and 3, has an energy of $E_{\text{adatom}} = -2.40$ eV.

IV. MONTE CARLO ANALYSIS

In principle, the energy surface $E_{\text{adatom}}(x,y)$ contains all the important physics of surface diffusion. A simple analysis

TABLE II. Activation energies, $\Delta E_{i,f}$, and hop rates, $r_{i,f}$, for the transitions from bonding site i to bonding site f . The activation energy $\Delta E_{i,f}$ is the difference between the binding energy at the initial site E_i and the binding energy $E_{\text{saddle}}^{i,f}$ at the saddle point between the initial and final sites: $\Delta E_{i,f} = E_{\text{saddle}}^{i,f} - E_i$. Since E_i is generally not equal to E_f , the activation energy for a hop from site i to site f is generally not equal to the activation energy for the hop going the other way. This explains why $\Delta E_{1,2}$ is not equal to $\Delta E_{2,1}$. Hops from site 1 to site 3 and vice versa are excluded because these sites are not adjacent. Parameters for Monte Carlo simulations using Vvedensky's harmonic oscillator approximation ($\nu_0 = 2kT/h$) are shown.

| Hop $i \rightarrow f$ | Activation energy $\Delta E_{i,f}$ (eV) | Hop rate in units of 10^9 s^{-1} $r_{i,f} = \nu_0 e^{-\Delta E_{i,f}/kT}$ |
|--------------------------|--------------------------------------------|----------------------------------------------------------------------------------------|
| 1 \rightarrow 2 | 0.33 | 5.4 |
| 2 \rightarrow 1 | 0.15 | 510 |
| 2 \rightarrow 3 | 0.45 | 0.33 |
| 3 \rightarrow 2 | 0.15 | 540 |

of such an energy surface yields the surface diffusion activation energies. These energies are simply defined as the difference between an energy minimum (a bonding energy) and a neighboring saddle point. Once determined, the activation energies can serve as input data for a kinetic Monte Carlo simulation, which in turn can produce effective diffusion coefficients and/or effective migration velocities. The kinetic Monte Carlo model makes two key assumptions. First, it is assumed that thermal equilibrium exists between the adatom and the underlying surface, and second, that microscopic reversibility (the principle of detailed balance) holds.² In Monte Carlo the migration of an adatom is modeled as a discrete site to site hopping process in which the rate for a hop from a given initial site i over a potential barrier to a final site f is assumed to have the Arrhenius form

$$r_{i,f} = \nu_0 e^{-\Delta E_{i,f}/kT}.$$

Here $\Delta E_{i,f}$ is the activation energy, i.e., the difference of the relative binding energies at the initial site E_i and the binding energy $E_{\text{saddle}}^{i,f}$ at the saddle point between the initial state i and the final state f . The attempt frequencies ν_0 are, according to transition state theory, related to the phonon modes at the binding sites and at the saddle points; however, it's computationally expensive to calculate these attempt frequencies from first principles.²⁹ Because the relevant phonon modes are not expected to vary much from site to site while the exponential term $e^{-\Delta E_{i,f}/kT}$ can easily vary by several orders of magnitude, we can approximate the attempt frequency as a site-independent constant without fear of losing the basic physics of the system. In this work we use Vvedensky's harmonic oscillator approximation for the attempt frequency: $\nu_0 = 2kT/h$, where k is Boltzmann's constant, h is Planck's constant, and T is the temperature in kelvin.³⁰ At 473 K this formula yields $\nu_0 \approx 2 \times 10^{13} \text{ s}^{-1}$. Most kinetic Monte Carlo models for surface diffusion and/or growth use similar site-independent approximations for the attempt frequencies.²

Table II shows the activation energies for the transitions from bonding site to bonding site. Using these data, we ran a kinetic Monte Carlo² simulation and have determined the adatom diffusion coefficients in directions parallel and per-

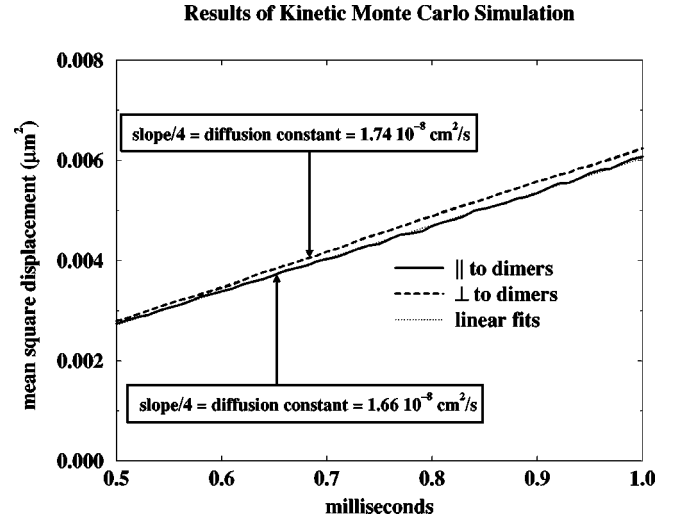


FIG. 3. Plot of mean squared displacement of the Ga adatom vs time. The results of our kinetic Monte Carlo simulations are shown. The mean squared displacement (averaged over 2000 runs) is shown as a function of time. The diffusion coefficient is equal to the slope of the linear fits to the data (dotted lines) divided by $2d$ (d being the dimension of system). Note that the diffusion coefficient in the direction perpendicular to the dimer rows D_{\perp} is very close to the value for the diffusion coefficient in the direction parallel to the dimer rows D_{\parallel} .

pendicular to the dimer rows. In the algorithm used here we assume that the Ga adatom sits in one of the three sites 1, 2, or 3, as specified above. The adatom can only make those hops specified in Table II. In our simulations, we chose a temperature consistent with that used in the low-temperature growth of GaAs: 473 K. Figure 3 shows the results of a kinetic Monte Carlo run performed using $\nu_0 = 2kT/h$. These results indicate that Ga adatom diffusion on this surface at 473 K is essentially symmetric with a diffusion coefficient $D_{\parallel} = 1.66 \times 10^{-8} \text{ cm}^2/\text{s}$ for motion parallel to the dimerization direction and $D_{\perp} = 1.74 \times 10^{-8} \text{ cm}^2/\text{s}$ perpendicular to the dimerization direction. The apparent symmetry of diffusion is somewhat surprising considering the significant asymmetry of the original Ga adatom potential energy map. However, a close examination of the routes for parallel and perpendicular diffusion yields the explanation. If an adatom is to hop from a site of type 1 to any of the four nearest-neighbor type 1 sites, it must first execute the three hops $1 \rightarrow 2 \rightarrow 3 \rightarrow 2$. However, having arrived at site 2, the adatom can either go to site 1 or site 3. Since the $2 \rightarrow 1$ barrier is about 1/3 the height of the $2 \rightarrow 3$ barrier, at 473 K the adatom is about 1500 times more likely to hop into site 1 (the hopping rates are $r_{2,1} = 510 \times 10^9 \text{ s}^{-1}$ and $r_{2,3} = 0.33 \times 10^9 \text{ s}^{-1}$). And since the path between site 1 nearest neighbors is at an angle of 45° to the dimer rows, the sequence $1 \rightarrow 2 \rightarrow 3 \rightarrow 2 \rightarrow 1$ takes the adatom the same distance both parallel and perpendicular to the dimer rows. The result is isotropic diffusion despite the anisotropic Ga adatom energy map.

It's important to note that the absolute values of the calculated diffusion coefficients are not expected to be particularly accurate due to the uncertainty of some of the underlying assumptions used in the kinetic Monte Carlo simulation, e.g., the use of site-independent attempt frequencies obtained

using Vvedensky's harmonic oscillator approximation.³⁰ However, since the physics of the Ga adatom diffusion does not depend sensitively on the details of our Monte Carlo model, this should not have much of an effect on the basic diffusion mechanism. Whatever reasonable approximations are used, the dominant diffusion pathways will continue to pass through site 1 due to the large ratio between $r_{2,1}$ and $r_{2,3}$, and for this reason diffusion will remain essentially isotropic.

V. CONCLUSION

We performed a large-scale *ab initio* investigation of Ga adatom diffusion on the GaAs(100)- $c(4\times 4)$ surface. The result of this calculation is a potential energy map for the Ga adatom over the whole surface. At first glance, this surface seemed to indicate that the Ga diffusion should be highly anisotropic, with the Ga adatoms freely traveling in the trough between the dimer rows but being hindered by large potential barriers and deep wells in the pathway through the missing dimer row. However, a kinetic Monte Carlo simula-

tion using our calculated data showed that this is not the case. In actuality, the Ga adatom is much more likely to fall into the well at site 1 than to continue along the trough between the dimer rows. As a result, Ga adatom diffusion on this surface is surprisingly isotropic.

ACKNOWLEDGMENTS

We thank K. Eyink, J. Pelz, and M. Seaford for useful discussions. This research was supported in part by the U.S. Department of Energy Basic Energy Sciences, Division of Materials Sciences, and by NSF Grant No. DMR-9520319. This research was conducted using the resources of the Cornell Theory Center, which receives major funding from the National Science Foundation (NSF) and New York State, with additional support from the Advanced Research Projects (ARPA), the National Center for Research Resources at the National Institutes of Health (NIH), IBM Corporation, and other members of the center's Corporate Partnership Program. We also acknowledge computer time on the IBM SP2 from the Ohio State Supercomputer Center.

-
- ¹See for instance, T. Irisawa, Y. Arima, and T. Kuroda, *J. Cryst. Growth* **99**, 491 (1990); J.M. McCoy and J.P. LaFemina, *Phys. Rev. B* **50**, 17 127 (1994).
- ²A number of reviews on this method have been written. See A. Madhukar and S.V. Ghaisis, *CRC Crit. Rev. Solid State Mater. Sci.* **14**, 1 (1988). For shorter introductions to the topic, see D.D. Vvedensky, T. Shitara, P. Smilauer, T. Kaneko, and A. Zangwill, in *Common Themes and Mechanisms of Epitaxial Growth*, MRS Symposia Proceedings No. 312 (Materials Research Society, Pittsburgh, 1988), p. 3.; A. Madhukar, *Surf. Sci.* **132**, 344 (1983).
- ³See for instance P. Smilauer and D.D. Vvedensky, *Phys. Rev. B* **48**, 17 603 (1993); T. Shitara *et al.*, *ibid.* **46**, 6825 (1992); J.M. McCoy and P.A. Maksym, *Semicond. Sci. Technol.* **6**, 141 (1991).
- ⁴T. Ito, K. Shiraishi, and T. Ohno, *Appl. Surf. Sci.* **82**, 208 (1994), and references therein.
- ⁵G. Brocks, P.J. Kelly, and R. Car, *Phys. Rev. Lett.* **66**, 1729 (1991) [*ab initio* pseudopotential Car-Parrinello calculation of Si adatom energy surface on Si(100)]; Kenji Shiraishi, *Appl. Phys. Lett.* **60**, 1363 (1992) [pseudopotential calculation of Ga adatom energy surface ($X\alpha$ potential for the electron exchange-correlation potential)]; A. Palma *et al.*, *J. Cryst. Growth* **150**, 180 (1995) [a parametrized Lifson-Warshel valence-force field calculation of Ga adatom on GaAs(001)].
- ⁶P.E. Blöchl, *Phys. Rev. B* **50**, 17 953 (1994).
- ⁷E. Wimmer, H. Krakauer, M. Weinert, and A.J. Freeman, *Phys. Rev. B* **24**, 864 (1981).
- ⁸D.R. Hamann, L.F. Mattheiss, and H.S. Greenside, *Phys. Rev. B* **24**, 6151 (1981).
- ⁹G.B. Bachelet, D.R. Hamann, and M. Schlüter, *Phys. Rev. B* **26**, 4199 (1982).
- ¹⁰J.P. Perdew and A. Zunger, *Phys. Rev. B* **23**, 5048 (1981).
- ¹¹R. Car and M. Parrinello, *Phys. Rev. Lett.* **55**, 2471 (1985).
- ¹²D. Remler and P. Madden, *Mol. Phys.* **70**, 921 (1990).
- ¹³M.C. Payne, M.P. Teter, D.C. Allan, T.A. Arias, and J.D. Joannopoulos, *Rev. Mod. Phys.* **64**, 1045 (1992).
- ¹⁴F. Tassone, F. Mauri, and R. Car, *Phys. Rev. B* **50**, 10 561 (1994).
- ¹⁵P. Margle, T. Ziegler, and P.E. Blöchl, *J. Am. Chem. Soc.* **117**, 12 625 (1995).
- ¹⁶P. Margl, K. Schwarz, and P.E. Blöchl, *J. Chem. Phys.* **103**, 683 (1995).
- ¹⁷P. Margl, K. Schwarz, and P.E. Blöchl, *J. Am. Chem. Soc.* **116**, 11 177 (1994).
- ¹⁸P. Margl, K. Schwarz, and P.E. Blöchl, *J. Chem. Phys.* **100**, 8194 (1994).
- ¹⁹N.A.W. Holzwarth, G.E. Matthews, R.B. Dunning, A.R. Tackett, and J. Zeng, *Phys. Rev. B* **55**, 2005 (1997).
- ²⁰Using a plane-wave cutoff of 30 Ry and a Brillouin zone integration scheme involving a regular grid of 64 k points in the complete Brillouin zone of the usual 2 atom fcc unit cell, the PAW method yielded a lattice constant for bulk GaAs of 5.61 Å, just 0.7% less than the experimental lattice constant and compares well with other calculations [see M. Alouani and J. M. Wills, *Phys. Rev. B* **54**, 2480 (1996) and references therein; Y. Juan, E. Kaxiras, and R.G. Gordon, *ibid.* **51**, 9521 (1995)].
- ²¹Test simulations indicated that using the experimental lattice constant is reasonable. The first test involved the construction of a three-dimensional analog of our two-dimensional surface unit cell. This unit cell consisted of 64 atoms arranged in a *cubic* bulk unit cell whose lattice vectors corresponded to the in-plane lattice vector of the $c(4\times 4)$ surface unit cell. For this calculation we used the same plane-wave cutoff (10 Ry) as used in the surface calculations and a regular grid of eight k points in the complete Brillouin zone (the four k -point vectors in the x - y plane are the same as those of the surface unit cell). This calculation produced a lattice constant of 5.646, just 0.07% less than the experimental lattice constant. In the second test, we calculated the energy difference of the adatom binding energies at sites 1 and 2 at the experimental and at the calculated (0.7% less than experiment, see Ref. 20) lattice constants. The energy dif-

- ference between sites 1 and 2 changed by only 10 meV, well within chemical accuracy (25 meV).
- ²²Private communication with Sverre Froyen. Using a plane wave cutoff of 10 Ry, the experimental lattice constant, and the k -point set used in the main calculation, we were able to duplicate the geometry supplied by Froyen. Froyen's calculations were performed using the same plane-wave cutoff (10 Ry). However, whereas our calculation was performed using the PAW method, Froyen used the pseudopotential method (Vanderbilt pseudopotentials). Froyen also used a significantly different lattice constant (4% less than the experimental value). More detail of Froyen's calculation can be found in J.E. Bernard, S. Froyen, and A. Zunger, *Phys. Rev. B* **44**, 11 178 (1991). In terms of reduced coordinates (the raw coordinates divided by the lattice constants used in the respective calculations) our coordinates deviated from those of Froyen by 0.6% on average. The maximum deviation is 2.4%.
- ²³The total energy of the the complete structure (surface plus a Ga adatom) varies over a range of 1.44 eV, depending on the position of the Ga adatom. Thus, an energy convergence criterion δE of 1 mH is just 2% of the range of energies seen in the Ga adatom potential energy map. Likewise, an energy convergence criterion δE of 0.01 mH is just 0.2% of the smallest site-to-site activation barrier (0.14 eV for the 3 \rightarrow 2 hop).
- ²⁴Many researchers terminate their simulations when the forces on the atoms fall below some pre-established smallness criterion $\delta \vec{F}$. However, the value below which a force can safely be considered to be negligible is intimately connected to the phonon spectrum and as such varies from system to system. By conducting a zero-friction run over a suitable time period, it can be directly verified that the system remains in the (suspected) ground-state configuration.
- ²⁵D.K. Biegelsen, R.D. Bringans, J.E. Northrup, and L.E. Swartz, *Phys. Rev. B* **41**, 5701 (1990).
- ²⁶J.E. Northrup and S. Froyen, *Phys. Rev. B* **50**, 2015 (1994), and references therein.
- ²⁷A.C. Warren, J.M. Woodall, P.D. Kirchner, X. Yin, F. Pollak, M.R. Melloch, N. Otsuka, and K. Mahalingam, *Phys. Rev. B* **46**, 4617 (1992).
- ²⁸M.R. Melloch, D.C. Miller, and B. Das, *Appl. Phys. Lett.* **54**, 943 (1989).
- ²⁹G.H. Vineyard, *J. Phys. Chem. Solids* **3**, 121 (1957).
- ³⁰We have used Clarke and Vvedensky's harmonic oscillator approximation for ν_0 , see S. Clarke and D.D. Vvedensky, *Phys. Rev. Lett.* **58**, 2235 (1987).